Vol. 14(3): 511-533, September 2026 DOI: https://doi.org/10.23960/jsl.v14i3.1531

Jurnal Sylva Lestari

P-ISSN: 2339-0913
E-ISSN: 2549-5747

Journal homepage: https://sylvalestari.fp.unila.ac.id

Full Length Research Article

Phytochemical Profiles and Cytotoxicity Activities of *Eucalyptus* Leaf Oils from *Eucalyptus* Clones

Rita Kartika Sari[1,2,*], Yanico Hadi Prayogo[1,2], Agus Purwoko[3], Anne Carolina[1], Elisa Ganda Togu Manurung[1], Gunawan Pasaribu[4]

[1] Department of Forest Products, Faculty of Forestry and Environment, IPB University, Bogor, Indonesia
[2] Tropical Biopharmaca Research Center, IPB University, Bogor, Indonesia
[3] Forestry Study Program, Faculty of Forestry, Universitas Sumatera Utara, Deli Serdang, Indonesia
[4] Research Center for Applied Botany, National Research and Innovation Agency (BRIN), Bogor, Indonesia
[*] Corresponding author. E-mail address: rita_kartikasari@apps.ipb.ac.id

ARTICLE HISTORY:

Received: 17 April 2026
Peer review completed: 31 May 2026
Received in revised form: 14 June 2026
Accepted: 27 June 2026

KEYWORDS:

A549 lung cancer cell lines
B16-F10 murine melanoma cell lines
Gas Chromatography–Mass Spectrometry
Molecular docking
Multivariate analysis

© 2026 The Authors. Published by the Department of Forestry, Faculty of Agriculture, University of Lampung. This is an open access article under the CC BY-NC license: https://creativecommons.org/licenses/by-nc/4.0/.

ABSTRACT

Although widely cultivated for wood production in Indonesia, studies on *Eucalyptus* leaf essential oils (ELEOs) from *Eucalyptus* clones remain limited. This study investigated the yield, phytochemical profiles, cytotoxic activities, and putative compounds associated with the cytotoxicity of ELEOs obtained from seven *Eucalyptus* clones cultivated in North Sumatra, Indonesia. The oils were extracted by water-and-steam distillation for 1.5 h, starting when the first oil droplet appeared. Phytochemical profiles were characterized by gas chromatography–mass spectrometry, and cytotoxicity against A549 lung cancer and B16-F10 murine melanoma cells was evaluated *in vitro*. Multivariate analyses, such as orthogonal partial least squares and principal component analysis, together with molecular docking, were used to identify compounds associated with cytotoxicity. Essential oil yield ranged from 0.15% to 0.39% (w/w), while eucalyptol, the principal quality marker of ELEO, ranged from 7.98% to 41.69% among the clones. The clone of *Eucalyptus grandis* × *Eucalyptus* open-pollinated clone (GOP) exhibited the lowest IC_{50} value for B16-F10 cells (165.3 µg/mL), and the clone of *E. urophylla* × *Eucalyptus* open-pollinated clone (UOP1) exhibited the lowest IC_{50} value for A549 cells (111.9 µg/mL). According to multivariate analyses and molecular docking, α-pinene, (–)-spathulenol, and (–)-globulol are compounds that likely exhibit cytotoxicity against B16-F10 cells, while γ-terpinene, *o*-cymene, *o*-cymen-5-ol, and leptospermone are compounds that likely exhibit cytotoxicity against A549 cells. However, in normal cell lines, it was not possible to achieve cytotoxic selectivity, as the biological significance of the observed cytotoxic responses is not yet established. In general, the results indicated that the yield, phytochemical composition, and cytotoxic activity of ELEOs derived from *Eucalyptus* clones depend on the genetic background.

1. Introduction

Eucalyptus trees are widely distributed in tropical regions, such as Indonesia, and are predominantly cultivated in industrial plantation forests (IPFs). *Eucalyptus* trees are productive and have high biomass in hybrid plantations (Marnaek et al. 2024), are used for soil amelioration

to improve growth on poor lands (Munawaroh et al. 2025), and are sensitive to seedling quality and planting (Ekamawanti et al. 2021). The main use of *Eucalyptus* trees in Indonesia is as a source of wood fiber for the pulp, paper, and textiles industries (Nirsatmanto et al. 2022), with production increasing from 2.7 million to 22.8 million m^3 between 2014 and 2024 (BPS-Statistics Indonesia 2014, 2024). However, timber harvesting results in substantial leaf biomass that is wasted. The leaves of *Eucalyptus urophylla* S.T. Blake*, E. grandis* W. Hill. Ex Maiden*, E. pellita* F. Muell.*,* and its unique clones contain *Eucalyptus* leaf essential oils (ELEOs) composed of various terpenoids, especially eucalyptol (1,8-cineole). Although the eucalyptol content in these clones (18–66%) is lower than the international pharmaceutical standard (≥ 70%), their chemical composition may provide other biological activities, considering possible uses in the pharmaceutical and healthcare sectors (Industry Research Ltd. 2025; Lu et al. 2014; Purwoko et al. 2024). Therefore, there is a high scientific and economic interest in the valorization of *Eucalyptus* leaves.

It has been scientifically proven that ELEOs are natural active ingredients with several biological activities, and the alternative valorization of the plants is supported. Eucalyptol-rich ELEO from *E. radiata* Sieber ex DC. (65.7% eucalyptol and 12.8% α-terpineol) is highly antibacterial against Streptococci and *Lactobacillus acidophilus* (Mahumane et al. 2016). Similarly, ELEO from *E. urophylla* containing 66.31% eucalyptol possesses potent antifungal activity against *Fusarium oxysporum and Aspergillus niger* (Pujiarti et al. 2018). Furthermore, ELEO from *E. grandis* × *E. urophylla* clone, despite its low eucalyptol (1.35 %). However, it was dominant α-pinene (17.02%) content, demonstrates moderate antioxidant activity, strong antibacterial activity against *Salmonella typhimurium,* and antifungal activity against *Colletotrichum gloeosporioides* (Zhou 2021). Other clonal ELEOs from *Eucalyptus* clones of *E. grandis* × *E. urophylla* and *E. grandis* × *E. pellita* (containing 31–41% eucalyptol, 21–42% α-pinene, and 2–5% α-terpineol) have shown significant efficacy against Gram-negative bacteria (*Klebsiella pneumoniae* and *S. typhi*) and Gram-positive bacteria (*Bacillus subtilis* and *Staphylococcus aureus*) (Prayogo et al. 2025).

The biological properties of ELEOs from pure *Eucalyptus* species have been extensively investigated, including their strong cytotoxic potential against lung and skin cancer cells. However, the cytotoxic activity of ELEOs derived from *Eucalyptus* clones has not yet been reported. Previous studies have shown that ELEO from *E. tereticornis* Sm. primarily composed of eucalyptol (34.39%) and iedol (9.92%), exerts strong cytotoxic activity against A549 lung cancer cell lines. In fact, *in silico* models suggested that five of its compounds possess better cytotoxic potential than the commercial lung cancer drug mobicertinib (Anju et al. 2023). Furthermore, ELEO of *E. camaldulensis* Dehnh. shows cytotoxic effects against A549 cells and WEHI-3 cells, and ELEO of *E. globulus* Labill. is cytotoxic to A549 cells and B16-F10 murine melanoma cell lines (Abiri et al. 2022). The results indicated that the cytotoxic effect of ELEOs is highly dependent on their phytochemical composition, which is greatly influenced by the tree species used, genetic crossing, and environmental growing conditions (Achmad et al. 2018).

In Indonesia, *E. urophylla, E. pellita,* and *E. grandis* clones are extensively used to grow IPFs in North Sumatera. They are significant genetic resources for plantation forestry in Indonesia because these clones have been developed for their improved growth performance, enhanced wood quality, and higher pest and disease resistance (Ekamawanti et al. 2021; Marnaek et al. 2024; Munawaroh et al. 2025). The chemical composition, physical properties (Alfian et al. 2019), and antimicrobial activities (Prayogo et al. 2025; Pujiarti et al. 2018) of essential oils of these particular

regional clones have been reported in previous studies. However, there is a lack of studies that investigate the intricate interplay between the specific phytochemical profile, the clonal genetic variation, and the resulting cytotoxic activity.

The discovery of natural anticancer compounds from these *Eucalyptus* clones is especially needed in Indonesia since the burden of cancer in Indonesia is very large. According to International Agency for Research on Cancer (2024), the number of new cancer cases experienced in Indonesia reached 408,661 people, and 242,988 people died from cancer. Lung cancer is the most common cancer killer and the second most common cancer. In addition, Indonesia is a tropical country with high ultraviolet (UV) rays and is witnessing a substantial number of skin cancer cases in the country, ranging from 2017 to 2022; the skin cancer cases reported were 5,245 cases (Bray et al. 2024). Traditional cancer treatments, such as chemotherapy, are also known for causing severe side effects as they affect healthy cells and are also known to trigger drug resistance. Consequently, plant-based phytochemicals such as essential gaining increasing interest as highly promising and effective alternatives that have fewer side effects. It has been shown that different phytochemicals in plants directly influence their biological and cytotoxic activities (Yip et al. 2024). Nevertheless, limited studies are reporting on the cytotoxic effects of ELEOs extracted from Indonesian *Eucalyptus* clones, and there is little evidence of the use of *in silico* approaches to predict their cytotoxic mechanisms (Prayogo et al. 2024).

The objectives of this study were to determine the ELEOs from seven *Eucalyptus* clones grown in North Sumatera, Indonesia, and their phytochemical components, as well as to evaluate their cytotoxic activity against A549 lung cancer cells and B16-F10 melanoma cells. The evaluated clones consisted of two *E. urophylla* × *E. pellita* crosses, one *E. grandis* × *E. urophylla* cross, one *E. urophylla* × *E. grandis* cross, two *E. urophylla* open-pollinated clones, and one *E. grandis* open-pollinated clone. In addition, multivariate analyses using orthogonal partial least squares (OPLS) and principal component analysis (PCA), together with molecular docking, were used to identify compounds associated with cytotoxic activity.

2. Materials and Methods

2.1. Plant Materials

Leaves were harvested from four-year-old *Eucalyptus* trees at the IPF of PT. Toba Pulp Lestari, Aek Nauli, North Sumatra, Indonesia. Seven *Eucalyptus* clones were studied (**Table 1**). For each clone, leaves were collected from nine randomly selected trees and grouped into three composite samples, each consisting of leaves from three trees. The leaves within each composite sample were mixed, air-dried for 24 h, and used as biological replicates in the subsequent analyses. Clone identity was confirmed using the breeding records and clone registration system of PT. Toba Pulp Lestari. The registered clone codes, maintained from nursery propagation through field establishment, served as the basis for sample collection.

2.2. Essential Oil Extraction and Yield Determination

The essential oils were extracted using a water-and-steam distillation system with a pilot-scale distillation unit (15 kg leaf capacity per batch). Freshly harvested leaves were air-dried under ambient conditions for 24 h. Subsequently, 10–11 kg of air-dried leaves with known moisture content were loaded into the distillation unit, and the process was continued for 1.5 h after the first

oil droplet appeared. The ELEOs were collected and stored at 4 °C. Essential oil yield (%) was calculated according to Purwoko et al. (2024) as the weight of essential oil obtained divided by the air-dried weight of leaves used for distillation and expressed as a percentage (w/w, air-dried leaf weight basis). The weight of essential oil was calculated from the measured oil volume using a density of 0.9165 g/mL, which falls within the density range specified for ELEO in ISO 3065 (2021) (0.906–0.925 g/mL at 20 °C). Samples were subsequently used for phytochemical and cytotoxicity analyses.

Table 1. Types of *Eucalyptus* clones used in the study

No	Clone number	Code of Clone	Parent	
			Female	Male
1	IND 73	UOP1	*E. urophylla*	Open pollination
2	IND 82	UOP2	*E. urophylla*	Open pollination
3	IND 83	UP1	*E. urophylla*	*E. pellita*
4	IND 58	UP2	*E. urophylla*	*E. pellita*
5	IND 68	GU	*E. grandis*	*E. urophylla*
6	IND 123	UG	*E. urophylla*	*E. grandis*
7	IND 116	GOP	*E. grandis*	Open pollination

2.3. Phytochemical Profiles Analysis

A GC–MS system (Agilent 7890 GC-5975 MSD, Agilent Technologies, USA) equipped with an RTX-5MS column (30 m × 0.25 mm × 0.25 µm) and helium (99.999%) as the carrier gas at a flow rate of 1.53 mL min^{-1} was used to analyze the chemical composition of ELEOs. For a total runtime of 27 minutes, the oven temperature was raised from 70 °C to 250 °C over 2 minutes. The split ratio was 10:1, the injection volume was 0.5 µL, and the injector temperature was set at 200 °C.

Mass spectrometry was performed in EI mode (70 eV) over the m/z 40–400 range. The temperatures of the ion source, quadrupole, and transfer line were set at 230, 150, and 250 °C, respectively. Agilent MSD ChemStation software (version E.02.02.1431, Agilent Technologies, Santa Clara, CA, USA) was used to process the data after it was collected in full scan mode. Compounds were identified via the NIST library. Literature retention index (RI) values for the identified compounds, obtained from studies using the same or similar GC columns (e.g., RTX-5MS), are provided in **Table 2** where available. Relative composition (%) was determined by peak-area normalization (semi-quantitative). Identified compounds were grouped into chemical classes (e.g., monoterpenes, oxygenated monoterpenes, and sesquiterpenes) based on their established terpenoid classification. All analyses were carried out in triplicate.

Multivariate analysis was performed using principal component analysis (PCA) in SIMCA software (version 14.1.0.2047, Umetrics, Sweden) to evaluate variations in phytochemical composition and to cluster samples. A total of 36 compounds, together with their relative abundances in each essential oil, were used as input variables for PCA. The PCA was performed using UV scaling without data transformation. The analysis was initially evaluated based on the first five principal components (PCs) generated.

The selection of PCs for further interpretation was based on their eigenvalues, with only PCs having eigenvalues greater than 1 retained according to Kaiser's rule. In total, the first five PCs

accounted for 90.9% of the variance. Specifically, PC1 and PC2 were selected to visualize variation among samples because they had the highest eigenvalues of 4.85 and 3.60, respectively.

2.4. In vitro Cytotoxicity Assay

The cytotoxic activity of ELEOs was evaluated using a resazurin-based cell viability assay (Susianti et al. 2021). B16-F10 melanoma and A549 human lung cancer cells were cultured in Roswell Park Memorial Institute (RPMI) medium (Gibco 11875-093) containing 10% fetal bovine serum (FBS) (Gibco 10270-106), and 1 µL/mL antibiotic (Sigma-Aldrich P4333) was added, and the samples were incubated at 37 °C and 5% CO_2 atmosphere (Thermo Scientific Series 8000DH).

For the assay, the cells (1.7×10^4 cells/well) were seeded into the 96-well plates and left to attach overnight, and incubated until about 70% confluence. Essential oil samples were prepared into stock solutions and then diluted in culture medium to get final concentrations of 31.25–500 µg/mL. Cells treated with culture medium containing 2% dimethyl sulfoxide (DMSO). The negative control was DMSO. Doxorubicin (30.07 µg/mL) and cisplatin (15.56 µg/mL) were used as positive controls for A549 and B16-F10 cells, respectively. Both positive controls were tested at only one reference concentration to monitor the performance of the assay and were therefore not subjected to IC_{50} determination.

The plate layout for the assay is shown in **Fig. 1.** All blanks were filled with culture medium. Cell control wells were filled with untreated cells, whereas only one well was filled with the treated cells. More well was given to the essential oils of various concentrations. Two wells were used for each concentration of sample (duplicate wells) in the same 96-well plate. The assay was performed twice independently on two separate 96-well plates to ensure the reproducibility of the observed reactions (Vaux et al. 2012).

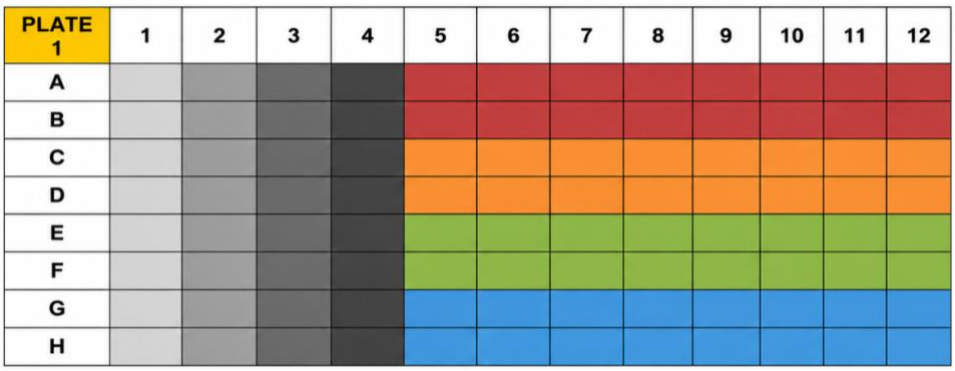

(a)

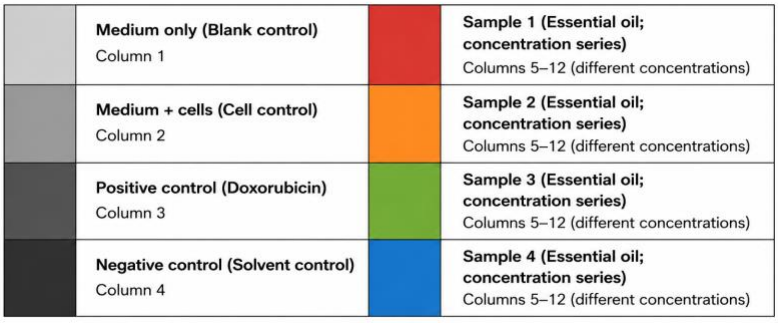

(b)

Fig. 1. Schematic layout of the 96-well plate for the cytotoxicity assay: (a) the arrangement of the plate and (b) legend of the control and treatment groups.

Cell attachment was followed by replacement of the media with fresh media containing either the test samples or the controls. These cells were then incubated for 48 h. Resazurin working solution was added to each well, and the mixture was incubated for 2 h at 37 °C. Cell viability was then determined by measuring absorbance at 570 nm with a reference wavelength of 600 nm using the Tecan Infinite M200 PRO instrument (Switzerland). Cell viability (CV) was calculated from the corrected absorbance values ($A_{570}-A_{600}$). The transformed cells were examined for morphological changes using an inverted microscope (EVOS XL Core; Thermo Scientific). Cell viability was expressed relative to the solvent control and used to construct concentration–response curves. IC_{50} values were calculated from the concentration–response curves and are the concentration needed to reduce the cell viability by 50%.

2.5. OPLS and Molecular Docking Analysis

The cytotoxicity test results were analyzed using IC_{50} values, which were calculated by nonlinear regression. The percentage of cancer cell survival as a function of the concentration of ELEO. The cytotoxic activities of ELEOs from each clone were assessed using multivariate analysis methods, including OPLS analysis with SIMCA 14.1.0.2047 software (Umetrics, Sweden). Identification of phytochemical compounds responsible for cytotoxicity against the B16-F10 and A549 cell lines was done using OPLS analysis.

A total of 36 phytochemical compounds were identified by GC-MS, along with their relative abundance values of the sample, and were used as X variables in the OPLS model. Cytotoxicity data (IC_{50} value) was used as the Y variable. The quality and reliability of the OPLS model were evaluated using R^2X, R^2Y, and Q^2. A permutation test of 200 permutations was used to assess the risk of model overfitting. In addition, CV-ANOVA was conducted to evaluate the statistical significance of the OPLS model. Bioactive compounds associated with cytotoxic activity were identified based on the YRelatedProfile values of the OPLS model. Compounds that show a strong association with cytotoxicity are thought to be potential phytochemical contributors to the observed cytotoxic response. The OPLS results were interpreted as exploratory evidence in favor of identifying compounds potentially associated with cytotoxic activity, rather than as definitive evidence of causal mechanisms.

Compounds that significantly contribute to cytotoxicity in the B16-F10 and A549 cell lines were studied using *in silico* molecular docking to elucidate their interactions with target proteins for skin and lung cancer treatment. The B-rapidly accelerated fibrosarcoma (BRAF-V600E) protein was selected as the target for skin cancer. For lung cancer, the epidermal growth factor receptor (EGFR) was selected. The crystal structure of the protein molecules was downloaded from the Protein Data Bank (https://www.rcsb.org/) using the PDB IDs 4mnf (BRAF-V600E) and 3poz (EGFR). The 3D structures of the molecules were downloaded from the PubChem database (https://pubchem.ncbi.nlm.nih.gov/). The receptor crystal structures were prepared by removing non-receptor molecules, including water molecules and ions. Missing atoms were repaired, polar hydrogens were added, and Kollman charges were assigned. The prepared receptors were then saved in PDBQT format.

The molecular structures of the ligands were generated using ChemBio3D Ultra 11.0 and were then prepared using AutoDockTools 1.5.6 by merging nonpolar hydrogens, assigning charges, defining rotatable bonds, and saving the structures in PDBQT format. The docking site was determined based on the position of the co-crystal ligand bound to the target protein. Docking

validation was performed by redocking the co-crystal ligand into the receptor binding site using AutoDockTools 1.5.6. The validation was conducted to ensure that the docking protocol could reproduce the native binding pose of the inhibitor. The docking protocol was considered valid when the root-mean-square deviation (RMSD) was below 2 Å.

The grid center values for BRAF-V600E were 7.023 (x), 17.704 (y), and -46.954 (z), while those for EGFR (3poz) were 18.746 (x), 31.832 (y), and 11.626 (z). In addition, molecular docking analysis was conducted using a 20 × 20 × 20 Å grid box size, an exhaustiveness of 8, and a spacing of 0.375 Å (Prayogo et al. 2024). Molecular docking was performed using AutoDock Vina (Eberhardt et al. 2021). The molecular docking results were visualized using Discovery Studio Visualizer v21.1.0.20298 (Biovia, United States). As a result of redocking analysis using the co-crystal ligand, the RMSD values for BRAF and EGFR receptors were 1.281 and 1.682 Å, respectively.

3. Results and Discussion

3.1. The Essential Oil Yield

Analysis of variance (ANOVA) showed that *Eucalyptus* leaf essential oil yield differed significantly among the clones ($p < 0.05$). The yields ranged from 0.15% to 0.38% (w/w). Although ANOVA showed an overall significant difference among clones, Duncan's multiple range test indicated that some clones were not significantly different from each other. The UG and GU clones produced the highest yields and did not differ significantly. Similarly, UOP2 (cd) and UP2 (cd) were not significantly different, whereas the GOP clone (a) produced the lowest yield but did not differ significantly from UP1 (ab) (**Fig. 2**). These results suggest that essential oil yield is influenced by clonal genetics, consistent with previous reports (Purwoko et al. 2024; Prayogo et al. 2025).

Although UOP1 and UP1 were obtained from the same crosses as UOP2 and UP2, their ELEO yields differed (**Fig. 2**). The observed differences in ELEO yield suggest that genetic variation among individual clones might play a role. In the UOP clones, this variation may stem from open pollination, which naturally introduces genetic variability. This means that different clones or plants may have distinct genetic combinations, which influence their phenotypic characteristics. This is in agreement with what has previously been observed in *E. globulus* where open pollination enables genetic variation to be affected by pollen from other sources (Faia et al. 2022). Nevertheless, differences in yield among the *E. urophylla* × *E. pellita* (UP) clones could be attributed to genetic variation. This genetic variation will affect gene expression and enzyme activity involved in terpene biosynthesis pathways, thereby altering ELEO yield and composition (Li et al. 2023).

Another finding in this study was that the yield of ELEO from the UG clone was not significantly different from that of the GU clone (**Fig. 2**), despite these clones being derived from reciprocal crosses (**Table 1**). The absence of a significant difference between the UG and GU reciprocal-cross clones suggests that reciprocal crossing had a limited effect on ELEO yield in this study. In a reciprocal mating study of *E. urophylla x E. camaldulensis* hybrids, maternal effects on growth traits were observed, but these effects did not necessarily extend to all traits (Zhu et al. 2017). Other studies have demonstrated that hybrid performance is influenced by complex genetic mechanisms, including non-additive effects, so maternal effects may not always be the main factor

(Van den Berg et al. 2015). Therefore, the equal ELEO yields of the UG and GU clones in this experiment may indicate that maternal effects on this trait are probably negligible. However, this finding is preliminary and requires further verification, as other factors, such as specific genetic interactions and environmental conditions, may also influence ELEO yield.

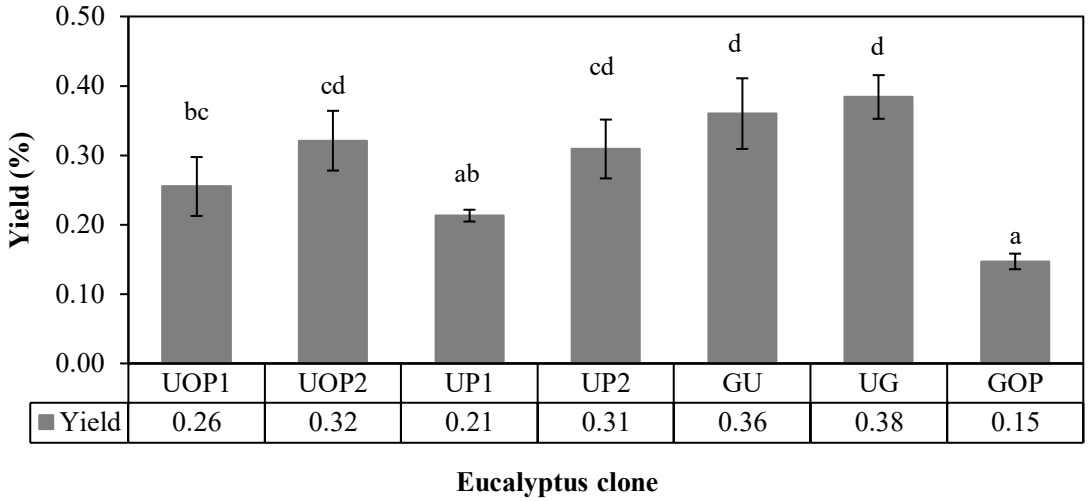

Fig. 2. Hydrodistillative yield of ELEOs (%) from *Eucalyptus* clones. Duncan's test indicates that bars with the same letter (or at least one common letter) do not differ significantly ($p < 0.05$).

3.2. Phytochemical Profile of Essential Oil

The ELEOs from different clones showed variability in their phytochemical profiles (**Table 2**). The UOP1, UOP2, UP2, UG, and GU clones contained high levels of eucalyptol phytochemicals, whereas the GOP clone showed high levels of α-pinene. Other phytochemicals, such as γ-terpinene, *o*-cymene, and *m*-cymene, also varied among the clones. This variation could be attributed to genetic and environmental factors (Bulama Modu et al. 2025; Prayogo et al. 2025; Rajapaksha et al. 2023). This difference can be observed in principal component analysis (PCA), with PC1 and PC2 accounting for 60.3% of the total variance. PCA separates the clones into four different chetypes (**Fig. 3a**). UOP1 and UOP2 exhibit similar chemical compositions. This is similar to the phenomenon observed in UG and GU. This grouping pattern is supported by loading plots that associate UOP1 and GOP with cymene and α-pinene compounds, respectively. Meanwhile, UOP2, GU, and UG with eucalyptol (**Fig. 3b**).

Although the yield of ELEO from the UG and GU clones was similar, their chemical compositions were quite different. Both clones contained similar amounts of eucalyptol. However, UG contained more α-pinene, and GU more γ-terpinene (**Table 2**). This is a compositional difference that might be attributable to variations in terpene biosynthetic pathways and genetic variation among clones (Rajapaksha et al. 2023; Zhou et al. 2021). This difference is also evident in the PCA score plot, indicating that the UG and GU are relatively close but do not completely overlap (**Fig. 3a**). The high percentage of eucalyptol indicates that they are very close together, implying similarity due to proximity. The loading plot (**Fig. 3b**) confirms that the clustering pattern is related to eucalyptol and D-limonene, and also to α-pinene and γ-terpinene. The results above show the difference in composition is likely related to the genetic regulation of terpene production, as previously reported in *Eucalyptus* (Lu et al. 2014; Zhou et al. 2021).

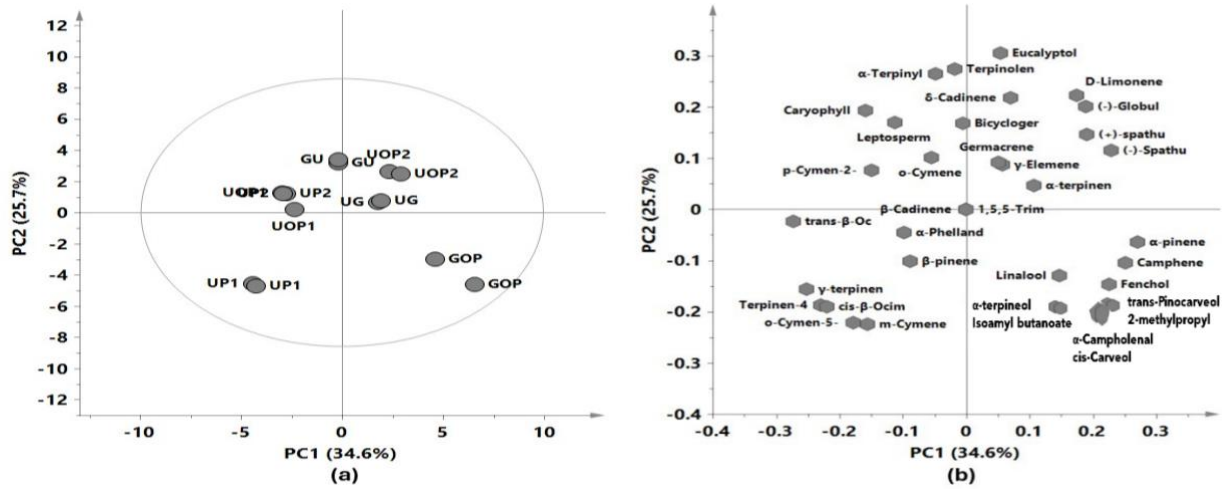

Fig. 3. Plot of score (a) and loading (b) refers to the phytochemical profiles of ELEOs from *Eucalyptus* clones.

The loadings plot (**Fig. 3b**) provides additional information on the classification by listing the individual compounds used in this differentiation. Specifically, UP1 contains cymene derivatives, GOP contains monoterpenes (e.g., α-pinene, linalool, fenchol, and *trans*-pinocarveol), and the UOP2–GU–UG cluster contains eucalyptol and D-limonene. Based on these results, it can be inferred that the observed variation in phytochemicals is most likely under genetic control via terpene biosynthesis. The genotype-related changes in chemical composition have been reported in the genus *Eucalyptus* (Lu et al. 2014; Zhou et al. 2021).

Table 2. The relative content of chemical compounds of ELEOs from various *Eucalyptus* clones

RT (min)	RRI	Tentatively identified compound	Chemical class	SI (%)	Relative abundance (%)						
					UOP1	UOP2	UP1	UP2	UG	GU	GOP
6.5	1034[a]	Eucalyptol	Oxygenated monoterpenes (OM)	98	32.75 ±2.65	37.19 ± 2.49	7.90 ± 0.63	33.34 ± 0.33	41.69 ± 1.06	41.42 ± 2.09	13.44 ± 5.53
3.0	941[a]	α-pinene	Monoterpene	95	4.78 ± 2.76	29.07 ± 1.30	11.61 ± 1.21	4.15 ± 0.63	26.51 ± 0.34	11.91 ± 8.42	41.8 ± 6.58
7.7	1058[a]	γ-terpinene	Monoterpene	97	20.92 ± 1.93	1.89 ±0.40	30.47 ± 4.40	21.24 ± 0.60	2.29 ± 0.69	15.79 ± 00.88	5.77 ± 0.77
8.4	-	*o*-Cymene	Monoterpene	97	10.20 ± 0.71	2.66 ± 1.88	0 ± 0	10.90 ± 0.77	3.66 ± 0.55	4.86 ± 3.49	9.49 ± 1.12
28.8	1323[b]	α-Terpinyl acetate	OM	91	8.92 ± 0.88	4.30 ± 0.08	0.84 ± 0.18	10.44 ± 0.28	7.44 ± 0.04	7.74 ± 2.48	1.26 ± 0.78
8.5	1005[b]	*m*-Cymene	Monoterpene	95	5.30 ± 0.28	0 ± 0	26.57 ± 3.19	5.41 ± 2.65	0 ± 0	0 ± 0	0 ± 0
6.3	1028[a]	D-Limonene	Monoterpene	97	4.40 ± 0.73	6.25 ± 0.39	2.63 ± 0.12	3.94 ± 0.05	6.28 ± 0.19	5.14 ± 0.28	4.13 ± 0.05
7.3	1047[c]	*trans*-β-Ocimene	Monoterpene	96	4.49 ± 0.45	1.69 ± 1.19	3.99 ± 0.81	3.91 ± 0.12	2.07 ± 0.05	2.42 ± 0.41	0.88 ± 0.03
23.8	1177[a]	Terpinen-4-ol	OM	97	1.90 ± 0.33	0.25 ± 0.18	5.82 ± 0.85	2.25 ± 0.02	0.47 ± 0.09	0.57 ± 0.41	0.23 ± 0.03
28.9	1191[a]	α-terpineol	OM	95	0 ± 0	0.78 ± 0.10	1.86 ± 0.21	0 ± 0	4.22 ± 0.16	0.76 ± 0.08	3.52 ± 0.93
17.8	1123[b]	α-Campholenal	OM	80	0 ± 0	0 ± 0	0 ± 0	0 ± 0	0.39 ± 0.02	0 ± 0	6.13 ± 1.65
28.8	1014[a]	α-terpinene	Monoterpene	91	0 ± 0	4.37 ± 0.19	0 ± 0	0 ± 0	0 ± 0	0 ± 0	1.52 ±0.16
5.4	1001[a]	α-Phellandrene	Monoterpene	91	0.80 ± 0.51	1.24 ± 0.12	1.55 ± 0.61	0.50 ± 0.02	0.24 ± 0.01	0.91 ± 0.24	0.27 ± 0.23
49.6	-	o-Cymen-5-ol	OM	94	0.08 ± 0.02	0 ± 0	1.60 ± 0.45	0.13 ± 0.09	0 ± 0	0 ± 0	0 ± 0
48.3	1577[a]	(-)-spathulenol	OM	99	0.80 ± 0.23	0.81 ± 0.57	1.06 ± 0.93	0.41 ± 0.03	0.65 ± 0.02	0.56 ± 0.40	1.20 ± 0.72
6.0	-	Isoamyl butanoate	Aliphatic ester	86	0 ± 0	0 ± 0	0 ± 0	0 ± 0	0 ± 0	0 ± 0	1.22 ± 0.45

RT (min)	RRI	Tentatively identified compound	Chemical class	SI (%)	Relative abundance (%)						
					UOP1	UOP2	UP1	UP2	UG	GU	GOP
36.1	-	cis-Carveol	OM	98	0 ± 0	0 ± 0	0 ± 0	0 ± 0	0 ± 0	0 ± 0	1.00 ± 0.35
23.6	1416[a]	Caryophyllene	Sesquiterpene	99	0.90 ± 0.44	0.42 ± 0.3	0.79 ± 0.21	0.59 ± 0.03	0.42 ± 0.05	0.67 ± 0.48	0.17 ± 0.04
26.3	-	*trans*-Pinocarveol	OM	87	0 ± 0	0 ± 0	0 ± 0	0 ± 0	0.41 ± 0.01	0 ± 0	0.90 ± 0.32
3.9	-	2-Methylpropyl isobutyrate	Aliphatic ester	83	0 ± 0	0 ± 0	0 ± 0	0 ± 0	0 ± 0	0 ± 0	0.94 ± 0.1
22.8	-	Fenchol	OM	98	0 ± 0	0.35 ± 0.25	0.22 ± 0.15	0 ± 0	0.71 ± 0.02	0 ± 0	0.68 ± 0.17
21.3	1102[a]	Linalool	OM	96	0.20 ± 0.02	0.27 ± 0.19	0 ± 0	0.15 ± 0.11	0 ± 0	0.15 ± 0.11	0.7 ± 0.08
3.6	945[a]	Camphene	Monoterpene	96	0 ± 0	0.32 ± 0.23	0.21 ± 0.04	0 ± 0	0.48 ± 0.02	0.11 ± 0.08	0.58 ± 0.12
7.9	-	*cis*-β-Ocimene	Monoterpene	97	0.20 ± 0	0 ± 0	0.62 ± 0.13	0.18 ± 0.01	0 ± 0	0.06 ± 0.02	0 ± 0
4.3	973[a]	β-pinene	Monoterpene	94	0 ± 0	0.17 ± 0.12	0.47 ± 0.11	0 ± 0	0.23 ± 0.01	0.13 ± 0.09	0 ± 0
32.3	1523[a]	δ-Cadinene	Sesquiterpene	96	0 ± 0	0.50 ± 0.36	0 ± 0	0 ± 0	0 ± 0	0.48 ± 0.34	0 ± 0
49.0	1300[a]	p-Cymen-2-ol	OM	94	0.15 ± 0.04	0 ± 0	0 ± 0	0.49 ± 0.14	0 ± 0	0 ± 0	0 ± 0
30.7	-	Germacrene B	Sesquiterpene	80	0.10 ± 0.02	0.48 ± 0.12	0 ± 0	0 ± 0	0 ± 0	0 ± 0	0 ± 0
47.2	-	(-)-Globulol	Oxygenated Sesquiterpene (OS)	99	0.30 ± 0.10	0.36 ± 0.26	0.28 ± 0.07	0.26 ± 0.02	0.42 ± 0	0.23 ± 0.16	0.37 ± 0.09
8.9	1089[a]	Terpinolene	Monoterpene	96	0.43 ± 001	0.28 ± 0.02	0.08 ± 0.02	0.25 ± 0.00	0 ± 0	0.3 ± 0.02	0 ± 0
30.7	-	Bicyclogermacrene	Sesquiterpene	95	0 ± 0	0 ± 0	0 ± 0	0.38 ± 0.02	0.37 ± 0.06	0.31 ± 0.02	0 ± 0
30.7	-	1,5,5-Trimethyl-6-methylenecyclohexene	Monoterpene	90	0 ± 0	0 ± 0	0.35 ± 0.09	0 ± 0	0 ± 0	0 ± 0	0.30 ± 0.03
30.7	-	γ-Elemene	Sesquiterpene	83	0 ± 0	0.42 ± 0.0.6	0 ± 0	0 ± 0	0.21 ± 0.3	0 ± 0	0 ± 0
32.3	1513[a]	β-Cadinene	Sesquiterpene	95	0.40 ± 0.05	0 ± 0	0 ± 0	0 ± 0	0 ± 0	0 ± 0	0 ± 0
50.5	-	Leptospermone	OS	99	0.30 ± 0.08	0 ± 0	0 ± 0	0.34 ± 0.03	0 ± 0	0.23 ± 0.01	0 ± 0

Notes: RT (retention time); SI (similarity index); Reported Retention Index (RRI) using RTX-5MS taken from: [a]Hudaib et al. (2007); [b]Fikry et al. (2024); [c]Hudaib et al. (2001).

3.3. Cytotoxic Activity of Eucalyptus Leaf Essential Oil

The *in vitro* cytotoxicity of ELEOs was assessed by evaluating their effects on mouse melanoma cells (B16-F10) and human lung cancer cells (A549). **Table 3** shows the viability of A549 and B16-F10 cells in control groups.

Table 3. Cell viability of the control groups used in the cytotoxicity assay

Control type	Treatment	A549 Cell Viability (%)	B16-F10 cell viability (%)
Cell control	medium + cells	102.52±5.17	99.84±0.50
Negative control	2% DMSO	100.00	100.00
Positive control	Doxorubicin (30.07 µg/mL)	49.51±20.63	–
Positive control	Cisplatin (15.56 µg/mL)	–	19.93±6.07

The cell and solvent controls had viability values near 100%, suggesting that the culture conditions and the 2% DMSO did not affect cell viability. In contrast, the positive controls substantially reduced cell viability. Doxorubicin decreased A549 cell viability to 49.51%, whereas cisplatin reduced B16-F10 cell viability to 19.93%. These clear responses confirm that the assay conditions were appropriate and reliable for evaluating the cytotoxic effects of ELEOs. A similar

assay design using cisplatin as a positive control for B16-F10 cells was previously reported by Susianti et al. (2021). Because doxorubicin and cisplatin were tested only at a single reference concentration, dose–response curves were not generated, and IC_{50} values were not determined for these positive controls.

ELEO treatment causes morphological changes consistent with cytotoxicity in the B16-F10 melanoma cancer cell line and A549-human lung cancer cell line (**Fig. 4)**. This is characterized by differences in the morphology of cells treated with ELEO versus the negative control (treatment with solvents used to dilute ELEO). ELEO at 500 µg/mL reduced cell density, as reflected in the cell viability value (CV) shown on each micrograph, and resulted in visible morphological changes compared to negative controls. These morphological changes are characterized by cell shrinkage, rounding, and discharge from the culture surface. The degree of this morphological change varied among the ELEOs tested, indicating the presence of different cytotoxicity properties among ELEOs. In A549 cells, oils from UOP2 and UG clones produce less pronounced morphological changes than from some other clones.

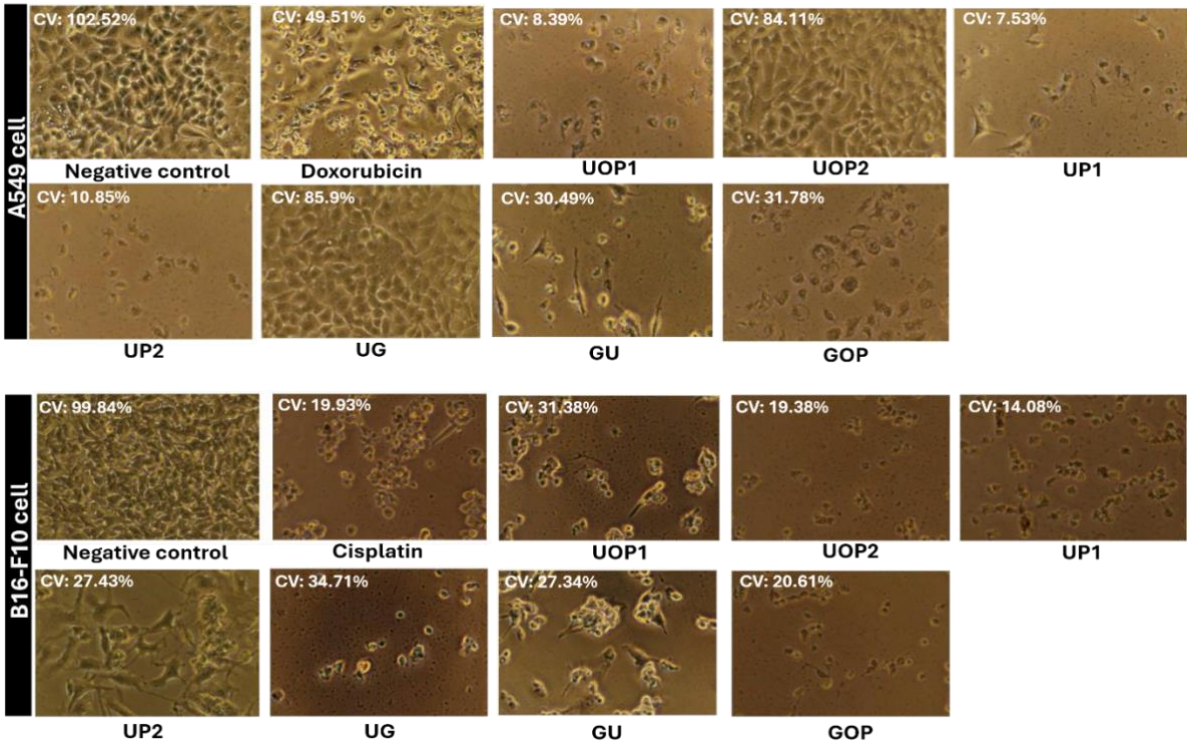

Fig. 4. Morphological changes of A549 and B16-F10 cells under negative control, positive control (doxorubicin for A549 cells and cisplatin for B16-F10 cells), and ELEO treatments (500 µg/mL). CV denotes cell viability (%).

The cytotoxic activity of ELEO varied between clones based on the IC_{50} value against B16-F10 cells and A549 cells. The ELEO of the GOP and UOP1 clones showed the lowest IC_{50} values against B16-F10 cells and A549 cells, respectively. Comparison of the two cell lines showed that the ELEO of UOP1 had a lower IC_{50} value in cells A549 than in cells B16-F10. An interesting phenomenon was observed that ELEO from *E. urophylla* × *E. pellita* (UP1 and UP2) and *E. grandis* × *E. urophylla* (UG and GU) crosses showed greater efficacy against B16-F10 cell lines than lung cancer cell lines A549 based on sensitivity ratio values. The E. *urophylla* clone produces oil that tends to be more toxic to A549 cells (indicated by a large ratio value), while the *E. grandis clone* produces oil that tends to be more toxic to B16-F10 cells. Although *the E. urophylla* clone

is able to produce the highest cytotoxicity, ELEO against A549 cells, not all ELEO from *the E. urophylla* clone exhibit the same cytotoxicity effect. This is observed in ELEO of UOP2 and UG that have an IC_{50} value greater than 500 µg/mL (**Table 4**). Therefore, these values suggest that the cytotoxic effects of this oil on A549 cells are limited under current experimental conditions.

Table 4. Cytotoxicity, expressed as IC_{50}, and Sensitivity ratio B16-F10/A549 of essential oils from *Eucalyptus* clones

Clone	IC_{50} (µg/mL)		Sensitivity ratio B16-F10/A549	Cell line preference
	B16-F10 cell line	A549 cell line		
UOP1	302.71	111.90	2.71	A549-sensitive
UOP2	316.22	>500.00	< 0.63	B16-F10-sensitive
UP1	492.50	302.71	1.63	A549-sensitive
UP2	398.11	316.23	1.26	slightly A549-sensitive
UG	204.80	>500.00	< 0.41	B16-F10-sensitive
GU	264.50	497.80	0.53	B16-F10-sensitive
GOP	165.30	398.10	0.42	B16-F10-sensitive

The observed differences among clones suggest that cytotoxic activity may be influenced by clonal variation and associated differences in phytochemical composition. This interpretation is supported by the statement of Lowman et al. (2018) that variations in the terpenoid profiles are important in cytotoxic activity. Similarly, Yip et al. (2024) reported that differences in the chemical composition of ELEOs from selected pure and hybrid species were closely associated with variations in their biological activities.

The stronger activity of the GOP clone against B16-F10 cells may be due to its higher α-pinene concentration. In contrast, the high activity of UOP1 against A549 cells may be associated with the presence of γ-terpinene, *trans*-β-ocimene, and terpinen-4-ol. The relative contents of these three compounds were comparatively high in UOP1, particularly *trans*-β-ocimene, which had the highest relative abundance among the ELEOs. A previous study reported that a *trans*-β-ocimene-rich essential oil exhibited cytotoxicity against SW-60 and MCF7 cells (Moriarity et al. 2007). However, to the best of our knowledge, no study has specifically evaluated the cytotoxicity of this compound against A549 cells. This composition-activity link is also supported by the results of the principal component analysis (PCA), which showed distinct chemotypes among clones (**Fig. 3a**). The pattern of clustering, which was not strictly along the parental line, suggests that interspecific hybridization plays a role in the establishment of different phytochemical profiles and associated activities (Abiri et al. 2022). Similarly, the composition-dependent cytotoxicity of *Eucalyptus* essential oils, such as *E. tereticornis*, against A549 cells (Anju et al. 2023) suggests that genetic background and chemical variability influence cytotoxicity. These results suggest that clonal variation dictates cytotoxic activity by altering chemical composition.

3.4. Prediction of Bioactive Compounds Based on Orthogonal Partial Least Squares Analysis and Molecular Docking

The prediction of cytotoxic activity for bioactive compounds was performed using orthogonal partial least squares (OPLS) and molecular docking to assess their potential to inhibit cancer cell growth. This approach enables initial evaluation of molecular interactions, biological activity, and potential mechanisms of action of the compounds across various cancer types. In this

study, the analysis focused on anti-skin-cancer and anti-lung-cancer activities to gain a more specific understanding of the potential cytotoxic activity of ELEOs.

3.4.1. Prediction of bioactive compounds for anti-skin cancer

In this study, phytochemicals exhibiting cytotoxic effects on B16-F10 cells were investigated. The OPLS model showed good explanatory and predictive performance, with $R^2X(cum)$, $R^2Y(cum)$, and $Q^2(cum)$ values of 0.509, 1.000, and 0.707, respectively. Model validation using permutation testing showed an R^2 intercept of 0.447 and a Q^2 intercept of −0.856, indicating that the predictive ability of the original model was not generated by random class assignment. In addition, the CV-ANOVA confirmed the model's statistical significance (*p*-value = 0.0166). From the OPLS analysis, various phytochemicals were found to be correlated with cytotoxicity against B16-F10 cells. The more negative the Y-related profile, the higher the probability of having a cytotoxic effect. A total of 36 compounds have been identified in ELEOs using OPLS analysis, with a Y profile < -0.4. It was predicted that *trans*-pinocarveol is the most potent phytochemical with cytotoxic activity against B16-F10 cells, followed by α-pinene, (–)-spathulenol, α-campholenal, D-limonene, 2-methylpropyl isobutyrate, camphene, *cis*-carveol, (–)-globulol, isoamyl butanoate, and eucalyptol, respectively (**Fig. 5**).

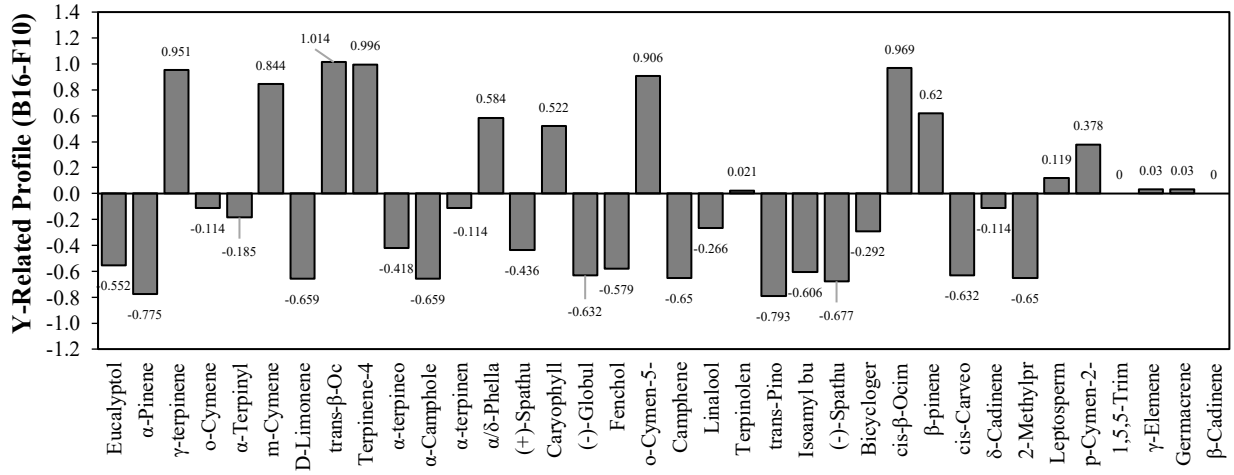

Fig. 5. Y-related profile values of phytochemical compounds in ELEO against the cytotoxicity of B16-F10 murine melanoma.

Among the OPLS-identified compounds, the sesquiterpene alcohol spathulenol has an IC_{50} of 11.67 µg/mL against the B16-F10 cell line (Bomfim et al. 2016). Similarly, α-pinene and camphene, both from the essential oil of *Piper cernuum* (Piperaceae), were shown to be active against the B16-F10 cell line with IC_{50} values of 24 and 70 µg/mL, respectively (Girola et al. 2015). Monoterpenoid alcohols such as *trans*-pinocarveol and *cis*-carveol have also shown moderate antiproliferative activity, including induction of oxidative stress and cell cycle arrest (Abiri et al. 2022; Anju et al. 2023). In contrast, ester compounds such as 2-methylpropyl isobutyrate and isoamyl butanoate have been rarely reported as the major cytotoxic compounds when isolated. However, they can indirectly affect cytotoxicity by increasing the permeability of the cell membrane to other terpenoids present in the essential oil extracts (Abiri et al. 2022; Anju et al. 2023). Given these data, it can be concluded that the cytotoxicity of ELEOs against B16-F10 cells may result from additive or synergistic effects among the terpenoids present in the mixture.

The cytotoxic activity against B16-F10 cells indicates the anti-melanoma potential of ELEOs. However, to predict the binding activity of compounds in ELEOs against clinically relevant melanoma-associated target proteins, the BRAF-V600E mutant was used in this study. B16-F10 cells are generally considered a BRAF wild-type murine melanoma cell line, and the V600 BRAF mutation, which is common in human melanoma, was not identified in the B16-F10 cell line (Zhong et al. 2020). Nevertheless, BRAF-V600E was selected as the docking target as an exploratory *in silico* approach to evaluate the potential interaction of bioactive compounds from ELEOs, because BRAF-V600E is a clinically relevant target in melanoma (Long et al. 2014). For BRAF-V600E, as one of the main protein targets of melanoma, (–)-spathulenol and (–)-globulol exhibited the best binding affinities due to their binding interactions (binding affinity of less than -7 kcal/mol) (**Fig. 6a**) and were able to form stable ligand-receptor complexes. However, the ligand-receptor interactions between the two compounds differed, with (–)-spathulenol exhibiting more interactions than (–)-globulol. Compounds (–)-globulol and (–)-spathulenol have different interactions with residue Phe583, with pi-sigma and alkyl interactions, respectively (**Fig. 6b** and **6c**), which are associated with ligand stability and might affect the inhibitory activity. Although both compounds showed high binding affinities, the phytochemicals in ELEOs exhibited lower binding affinities than the anticancer drug vemurafenib and the co-crystal ligand. In contrast, the major compound in ELEOs, eucalyptol, showed low binding affinity and interaction, indicating that the abundance of the compound in a mixture is not necessarily related to bioactivity. This result is in line with previous studies that indicated the importance of the bioactive component rather than the relative abundance (Anju et al. 2023; Zhou et al. 2021).

The ELEO from the GOP clone was the most cytotoxic against B16-F10 cells. The OPLS model suggested that α-pinene, the major component (41.8%) of the ELEO from GOP (**Table 2**), is the second-most-active compound with cytotoxic activity against B16-F10 cells. This predicted activity is in line with previous reports that α-pinene can activate natural killer (NK) cells (Jo et al. 2021), regulate miR-221 and induce G2/M phase cell cycle arrest (Xu et al. 2018), trigger apoptosis through caspase activation (Hou et al. 2019), and downregulate cisplatin-induced toxicity via the NRF2 pathway, while having low cytotoxicity to normal cells (de Barros et al. 2023; Demir et al. 2024). These results indicate that the cytotoxic activity is probably driven by α-pinene, in agreement with the OPLS model. However, molecular docking revealed that only (–)-globulol and (–)-spathulenol exhibited high affinity (≤ −7 kcal/mol) with the BRAF-V600E protein. This strong binding affinity indicates that both compounds may have potential as cytotoxic bioactive compounds against human melanoma cells harboring BRAF mutations. The OPLS results reflect the combined effects of multiple compounds in a multivariate system, whereas docking is based on binding to a single protein (BRAF-V600E). Therefore, major components (e.g., α-pinene) may exert their effects through other mechanisms, while minor components with high binding affinity may contribute to target-specific binding. In particular, α-pinene may contribute to the observed cytotoxic activity through multiple cellular mechanisms, including the modulation of oxidative stress and signaling pathways, rather than solely through direct binding to BRAF-V600E. These results support the concept that essential oil cytotoxicity relies on a multi-component, synergistic mechanism (Abiri et al. 2022; Anju et al. 2023; Yip et al. 2024).

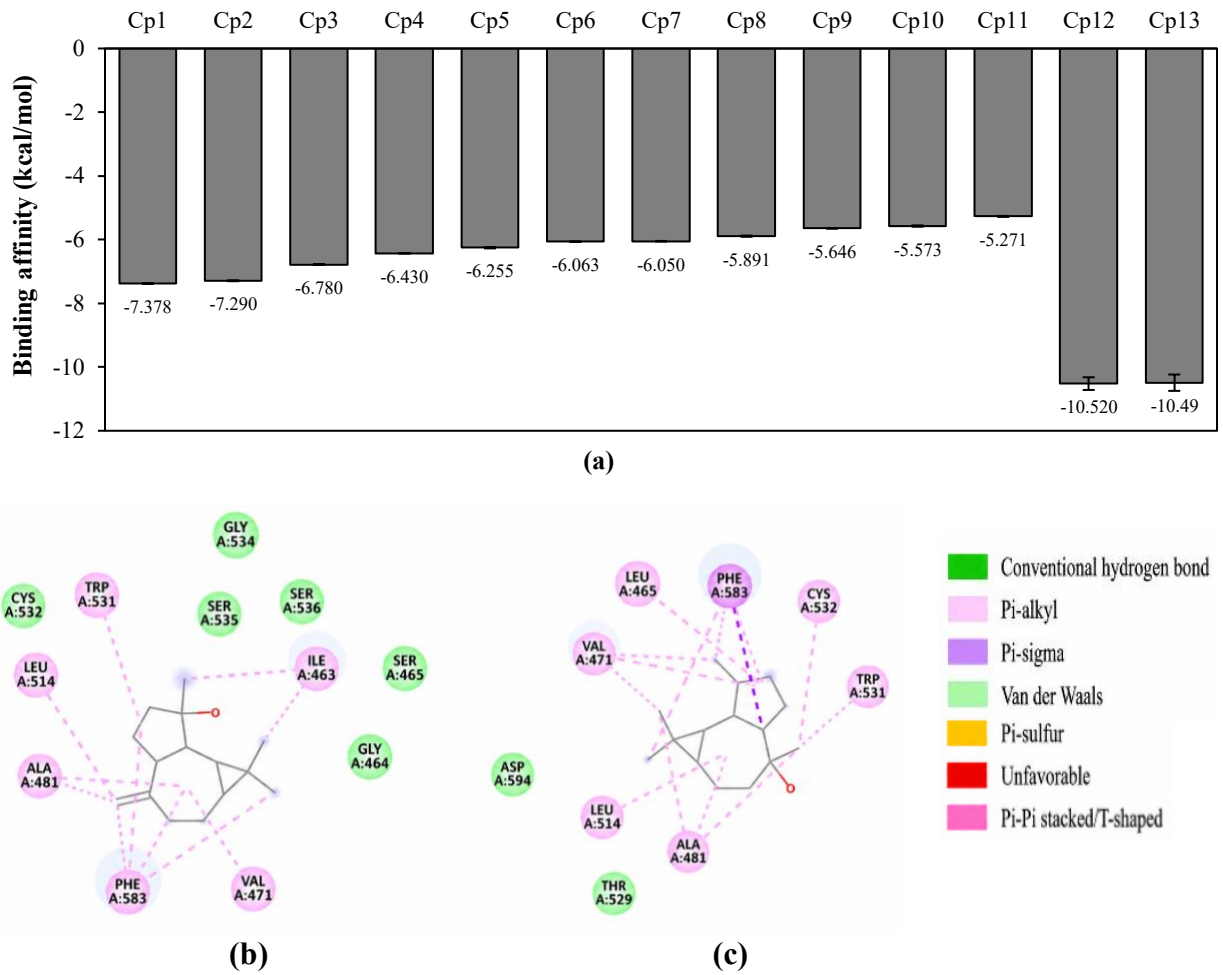

Fig. 6. Binding affinity of selected compounds against BRAF-V600E (a) and the interactions of two best docked compounds, (-)-spathulenol (b) and (-)-globulol (c). The compounds evaluated in this study were Cp1 ((-)-Spathulenol), Cp2 ((-)-Globulol), Cp3 (cis-Carveol), Cp4 (D-Limonene), Cp5 (α-Campholenal), Cp6 (α-Pinene), Cp7 (Camphene), Cp8 (trans-Pinocarveol), Cp9 (Eucalyptol), Cp10 (Isoamyl butanoate), Cp11 (2-Methylpropyl isobutyrate), Cp12 (Vemurafenib), and Cp13 (Co-crystalized ligand).

3.4.2. Prediction of bioactive compounds for anti-lung cancer

The OPLS model for A549 cells showed good explanatory and predictive performance, with $R^2X(cum)$, $R^2Y(cum)$, and $Q^2(cum)$ values of 0.502, 1.000, and 0.757, respectively. The predictive component explained 24.3% of the X variation and had an eigenvalue of 3.41, while the orthogonal component explained 25.9% of the X variation with an eigenvalue of 3.62. Model validation using permutation testing showed an R^2 intercept of 0.470 and a Q^2 intercept of −0.870. The negative Q^2 intercept indicates that the predictive ability of the original model was not generated by random permutation and supports the absence of strong overfitting. Furthermore, the CV-ANOVA confirmed the model's statistical significance (*p*-value = 0.0076). Therefore, the OPLS model was deemed sufficiently robust to support the exploratory identification of phytochemical compounds associated with cytotoxicity against A549 cells.

The results of the OPLS analysis showed that the compounds predicted to have anti-lung cancer activity in A549 cells (**Fig. 7**) were γ-terpinene, *trans*-β-ocimene, *p*-cymen-2-ol, *o*-cymene, terpinen-4-ol, *cis*-β-ocimene, *o*-cymen-5-ol, *m*-cymene, leptospermone, and α-phellandrene.

These compounds had varied relative abundances. Specifically, γ-terpinene, *o*-cymene, and *m*-cymene had high relative abundances in several ELEOs, whereas the other compounds showed low relative abundance (**Table 2**). A literature review indicates that γ-terpinene and terpinen-4-ol, isolated from camphor oil, exhibited cytotoxicity against the A549 human lung cancer cell line, with IC_{50} values of 21.50 and 86.83 µg/mL, respectively (Wu et al. 2016). In addition, ELEOs from *E. tereticornis* and *E. globulus* leaves also showed cytotoxic activity against lung cancer cells (Adnan 2019; Anju et al. 2023). Chemical analysis revealed that γ-terpinene, *o*-cymene, and *m*-cymene were present in relatively high proportions in these oils, supporting their predicted contribution to cytotoxicity. Consequently, the compounds predicted to exhibit anti-lung-cancer activity and to serve as putative marker compounds for ELEOs are γ-terpinene, *o*-cymene, and *m*-cymene.

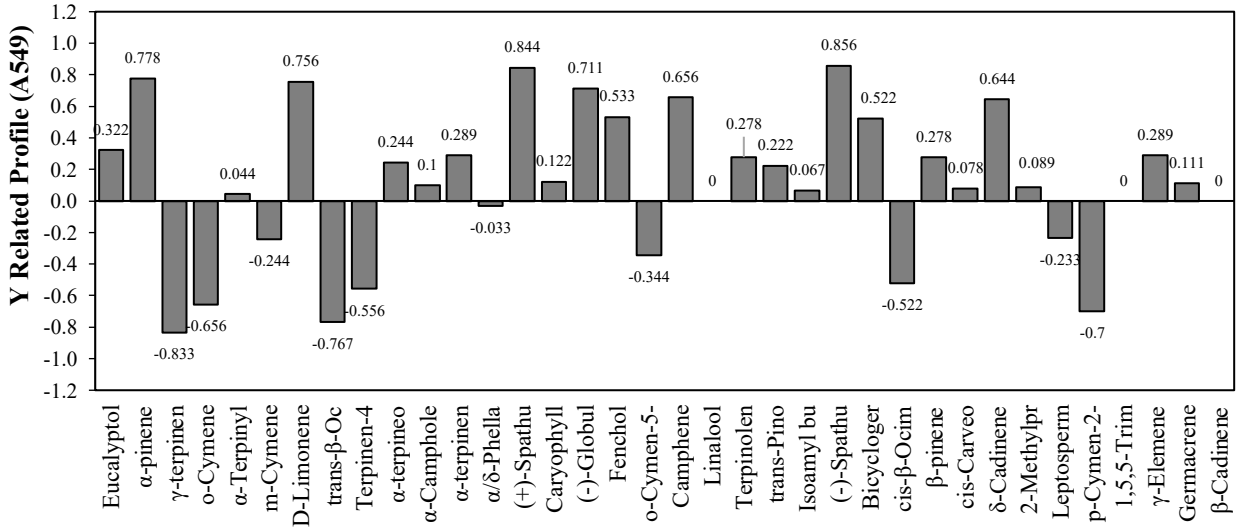

Fig. 7. Y-related profile values of phytochemical compounds in ELEO against the cytotoxicity of A549 human lung cancer cell lines.

Molecular docking analysis showed that compounds in ELEOs bound to the EGFR protein, a target in lung cancer, with binding affinities ranging from −5 to −7 kcal/mol. In general, these binding affinity values were still lower than those of the anticancer compound gefitinib and the co-crystal ligand of EGFR (**Fig. 8a**). The compound leptospermone (a sesquiterpene) achieved the best binding affinity, followed by *o*-cymen-5-ol (a monoterpene). These two compounds formed different interactions with the EGFR protein. Specifically, *o*-cymen-5-ol formed a π-π T-shaped interaction with Phe856 and a π-sigma interaction with Leu277, which were not observed in the interactions of leptospermone. Both compounds additionally formed hydrogen bonds with different amino acid residues, involving Met766 for *o*-cymen-5-ol and Lys745 for leptospermone, which stabilized the ligand-receptor interactions (**Figs. 8b** and **8c**). Some minor compounds showed stronger binding interactions than major compounds, such as eucalyptol, suggesting that the major compounds may not be solely responsible for the biological activity. This finding agrees with previous reports that minor constituents of essential oils can play an important role in biological activity through synergistic effects (Abiri et al. 2022; Anju et al. 2023).

The ELEO extracted from the UOP1 clone showed the highest cytotoxicity against the A549 human lung cancer cell line (**Table 3**). This ELEO from UOP1 contains higher *trans*-β-Ocimene than ELEOs from other clones. In addition, it contains other compounds that contribute to its high

anti-lung cancer activity, such as γ-terpinene, *p*-cymen-2-ol, *o*-cymene, terpinen-4-ol, *cis*-β-ocimene, *o*-cymen-5-ol, *m*-cymene, leptospermone, and α-phellandrene (**Fig. 7**). γ-Terpinene and terpinen-4-ol have been previously reported to have anticancer activity against A549 cells (Wu et al. 2016). Moreover, the ELEOs from *Eucalyptus* species (*E. tereticornis* and *E. globulus*) that contain these compounds also demonstrate cytotoxicity against lung cancer cells (Anju et al. 2023). These combined findings indicate that these compounds could be responsible for the observed cytotoxic activity.

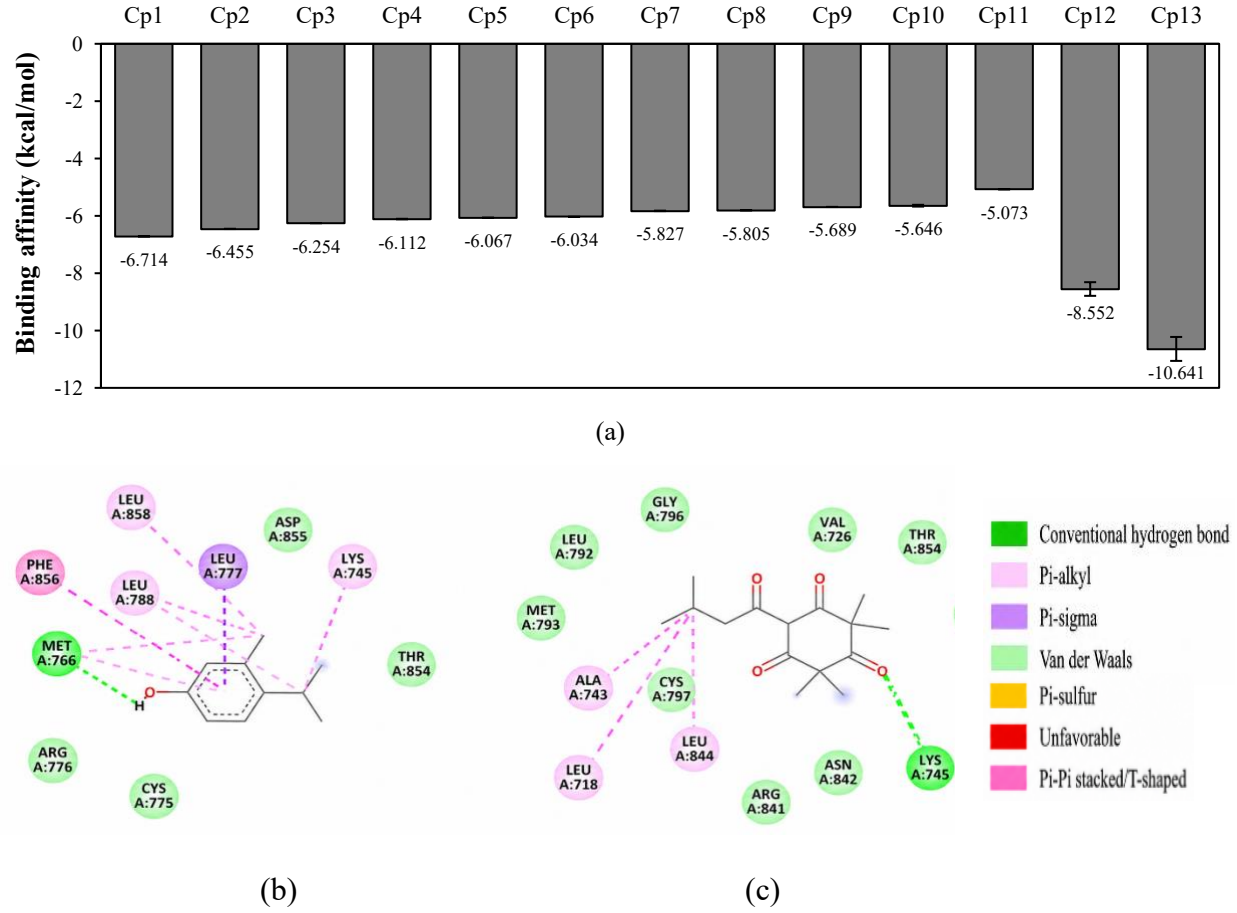

Fig. 8. Binding affinity of selected compounds against EGFR (a) and the interactions of the two best docked compounds, o-cymen-5-ol (b) and leptospermone (c). The compounds evaluated in this study were Cp1 (Leptospermone), Cp2 (*o*-Cymen-5-ol), Cp3 (p-Cymen-2-ol), Cp4 (Terpinen-4-ol), Cp5 (*m*-Cymene), Cp6 (*o*-Cymene), Cp7 (α-Phellandrene), Cp8 (γ-Terpinene), Cp9 (*trans*-β-Ocimene), Cp10 (cis-β-Ocimene), Cp11 (Eucalyptol), Cp12 (Gefitinib), and Cp13 (Co-crystal).

Table 2 illustrates that eucalyptol, also known as 1,8-cineol, was the main chemical component of ELEOs in almost all clones, except UP1 and GOP, with relative concentrations ranging from 32.73% to 41.69%. In contrast, ELEOs obtained from clones UP1 and GOP contained only about 7.98% and 13.44% of eucalyptol, respectively. Differences in the composition of essential oils can be caused by genetic differences among clones and by environmental factors that affect the yield and chemical profile of ELEOs (Bomfim et al. 2016; Wu et al. 2016; Yip et al. 2024). Previous studies have indicated that the eucalyptol content of *E. sideroxylon* leaf essential oil is 72–87%, depending on the harvest season (Koursaoui et al. 2021).

The production of ELEOs through crossbreeding *E. urophylla* with *E. pellita* or open pollination results in ELEOs with lower eucalyptol levels compared to ELEOs from its parent tree, *E. urophylla*. The eucalyptol content in ELEOs derived from *E. urophylla*, originating from the Wanagama I Educational Forest in Gunung Kidul, Yogyakarta, Indonesia, amounts to 49.86% (Pujiarti et al. 2018). **Table 2** showed that crossbreeding *E. grandis* with *E. urophylla* (UG and GU) produced ELEOs with the highest eucalyptol content. This is different from the chemical composition of ELEOs in the parent tree. The ELEOs from *E. grandis* were derived from the IPF of PT. Toba Pulp Lestari contained a higher amount of α-pinene (45.21%) than eucalyptol (36.55%) (Alfian et al. 2019). These findings indicate that ELEOs derived from crossbred *Eucalyptus* trees have a chemical composition different from that of the ELEO from the parent tree.Eucalyptol is the primary constituent of ELEOs and is recognized for its pharmacological properties, making it an effective therapeutic agent for respiratory diseases. Specifically, it exhibits anti-inflammatory effects. Eucalyptol can lower superoxide dismutase (SOD) expression and boost IL-10 levels in the airways of mice exposed to methyl methacrylate (MMA) vapor. Clinical trials have shown that eucalyptol is effective in treating asthma and rhinosinusitis. Eucalyptol has also been shown to exhibit cytotoxicity against leukemia, colon, breast, liver, and ovarian cancer (Cai et al. 2021). Other minor compounds in ELEOs, such as α-pinene, camphene, (–)-spathulenol, and *o*-cymen-5-ol, have also demonstrated cytotoxic and apoptotic activities *in vitro* and *in silico*, highlighting the contribution of major and minor components to the overall bioactivity of ELEOs (Abiri et al. 2022; Anju et al 2023; Wu et al. 2016). As such, eucalyptol is considered a key determinant of ELEOs' quality (ISO 3065 2021). However, the seven ELEOs studied in this research did not meet the ELEO quality standard because their eucalyptol content was below 60%, thereby reducing their market value or rendering them unsellable. The findings from this study may provide candidate compounds for further anti-skin and anti-lung cancer screening. Therefore, the ELEOs from the PT. Toba Pulp Lestari crossbred clones need to be created as a promising source of bioactive compounds by fractionating the ELEO and isolating the dominant compounds, which can then be further developed into cytotoxic agents.

Some limitations should be noted. Normal cell lines were not included in the cytotoxicity assay; therefore, Selectivity Index values could not be determined. In addition, doxorubicin and cisplatin were evaluated at a single reference concentration, and their IC_{50} values were not determined, thereby limiting direct comparison of the cytotoxic potency of the essential oils with that of standard anticancer drugs. In addition, retention indices were not determined during the GC–MS analysis, and compound identification was based mainly on NIST mass spectral matching, with literature RI values included when available. Furthermore, the OPLS analysis was performed with a limited number of clones (n = 7), and the results should therefore be interpreted as exploratory and used primarily to identify putative compounds associated with cytotoxicity.

4. Conclusions

The results showed significant differences among *Eucalyptus* clones in essential oil (ELEO) yields. Distinct phytochemical profiles were also observed among clones. Eucalyptol, the principal quality marker of ELEO, was the predominant constituent in most clones, whereas GOP and UP1 represented distinct chemotypes dominated by α-pinene and γ-terpinene, respectively. The differences were correlated with the differences in the cytotoxic responses against B16-F10 melanoma cells and A549 lung cancer cells. The ELEO from the GOP clone had the lowest IC_{50}

value against the B16-F10 melanoma cells, while the UOP1 clone had the lowest IC_{50} value against A549 lung cancer cells among the ELEOs evaluated. The cytotoxicity was associated with the presence of some terpenes (α-pinene, (−)-spathulenol, and (−)-globulol) in the phytochemical and chemometric analyses against B16-F10 cells. The molecular docking experiments provided further supporting evidence of potential interactions between certain chemicals (oxygenated sesquiterpenoids and monoterpenes) and target proteins associated with melanoma and lung cancer. However, they had lower binding affinities than their respective co-crystal ligands and reference compounds. This is a limitation of this study as cytotoxicity was tested only in cancer cell lines, and several oils exhibited only weak-to-moderate cytotoxicity. In addition, the proposed bioactive compounds were identified using multivariate analysis (limited by a small sample size of 7 clones) and molecular docking, without experimental validation. Further studies involving compound isolation, selectivity testing, and *in vivo* evaluation are needed to confirm these findings.

Acknowledgments

The authors would like to express their sincere gratitude to PT Toba Pulp Lestari Tbk. for providing access to the study site and facilitating sample collection, transportation, and accommodation; to the Faculty of Forestry, Universitas Sumatera Utara for providing a portable distillation unit; and to the National Research and Innovation Agency (BRIN) for providing access to the GC–MS analysis under the ELSA Point research service scheme, utilizing the service allocation of one of the authors.

Author Contributions

R.K.S., A.P., and G.P.: Conceptualization and project administration; R.K.S., A.P., and E.G.T.M.: Resources; R.K.S., Y.H.P., and A.C.: Methodology; R.K.S., A.C., and Y.H.P.: Software; R.K.S. and Y.H.P.: Validation; R.K.S. and Y.H.P.: Formal analysis; R.K.S., A.P., G.P., and E.G.T.M.: Investigation; R.K.S. and Y.H.P.: Data curation; Y.H.P., R.K.S., and A.C.: Writing original draft preparation; Y.H.P. and R.K.S.: Writing review and editing; R.K.S. and Y.H.P.: Visualization; R.K.S., A.P., and G.P.: Funding acquisition. All authors have read and agreed to the published version of the manuscript.

Conflict of Interest

The authors declare no conflict of interest.

Declaration of Generative AI and AI-Assisted Technologies in the Manuscript Preparation

Not applicable.

References

Abiri, R., Atabaki, N., Sanusi, R., Malik, S., Abiri, R., Safa, P., Shukor, N. A., and Abdul-Hamid, H. 2022. New Insights into the Biological Properties of *Eucalyptus*-Derived Essential Oils: A Promising Green Anticancer Drug. *Food Review International* 38(S1): 598–633. DOI: 10.1080/87559129.2021.1877300

Achmad, H. N., Rana, H. E., Fadilla, I., Fajar, A., Manurung, R., and Abduh, M. Y. 2018. Determination of Yield and Chemical Composition of Eucalyptus Oil from Different Species and Locations in Indonesia. *Biological and Natural Resources Engineering Journal* 1(1): 36–49. DOI: 10.31436/cnrej.v1i1.22

Adnan, M. 2019. Bioactive Potential of Essential Oil Extracted from the Leaves of *Eucalyptus globulus* (*Myrtaceae*). *Journal of Pharmacognosy and Phytochemistry* 8(1): 213–216.

Alfian, Z., Marpaung, H., Taufik, M., Lenny, S., Andriyani, and Samosir, S. J. 2019. GC-MS Analysis and Physical Properties of *Eucalyptus grandis* Essential Oil from PT Toba Pulp Lestari. *Asian Journal of Chemistry* 31(10): 2319–2322. DOI: 10.14233/ajchem.2019.21620

Anju, Kumar, A., Yadav, P., Navik, U., and Jaitak, V. 2023. Chemical Composition and Anticancer Evaluation of *Eucalyptus tereticornis* Leaf Essential Oil. *Natural Product Research* 37(10): 1656–1661. DOI: 10.1080/14786419.2022.2107642

BPS-Statistics Indonesia. 2015. *Statistics of Timber Culture Estates 2014*. BPS-Statistics Indonesia, Jakarta, Indonesia.

BPS-Statistics Indonesia. 2025. *Statistics of Timber Culture Estates 2024*. BPS-Statistics Indonesia, Jakarta, Indonesia.

Bomfim, L. M., Menezes, L. R., Rodrigues, A. C., Dias, R. B., Gurgel Rocha, C. A., Soares, M. B., Neto, A. F., Nascimento, M. P., Campos, A. F., Silva, L. C., et al. 2016. Antitumour Activity of Microencapsulated *Annona vepretorum* Essential Oil. *Basic and Clinical Pharmacology and Toxicology* 118(3): 208–213. DOI: 10.1111/bcpt.12488

Bray, F., Laversanne, M., Sung, H., Ferlay, J., Siegel, R. L., Soerjomataram, I., and Jemal, A. 2024. Global Cancer Statistics 2022: GLOBOCAN Estimates of Incidence and Mortality Worldwide for 36 Cancers in 185 Countries. *CA: ACancer Journal for Clinicians* 74(3): 229–263. DOI: 10.3322/caac.21834

Bulama Modu, M., Hanoğlu, D. Y., Hanoğlu, A., Alkaş, F. B., Başer, K. H. C., and Özkum Yavuz, D. 2025. Multivariate Statistical Analyses of the Temporal Variation in the Chemical Composition of the Essential Oil of *Eucalyptus torquata* in Cyprus. *Molecules* 30(2): 332. DOI: 10.3390/molecules30020332

Cai, Z. M., Peng, J. Q., Chen, Y., Tao, L., Zhang, Y. Y., Fu, L. Y., Long, Q. D., and Shen, X. C. 2021. 1,8-Cineole: Sources, Biological Activities, and Applications. *Journal of Asian Natural Products Research* 23(10): 938–954. DOI: 10.1080/10286020.2020.1839432

de Barros, D. B., Lima, E. O., da Silva, L. A., Fonseca, M. C., Ferreira, R. C., Diniz Neto, H., Alves, D. N., da Silva Rocha, W. P., Scotti, L., Lima, E. O., et al. 2023. α-Pinene: Docking Study, Cytotoxicity, Mechanism of Action, and Anti-Biofilm Activity Against *Candida albicans*. *Antibiotics* 12(3): 480. DOI: 10.3390/antibiotics12030480

Demir, S., Mentese, A., Usta, Z. T., Alemdar, N. T., Demir, E. A., and Aliyazicioglu, Y. 2024. α-Pinene Mitigates Cisplatin-Induced Reproductive Toxicity in Male Rats via Activation of the NRF2 Pathway. *International Urology and Nephrology* 56: 527–537. DOI: 10.1007/s11255-023-03817-5

Eberhardt, J., Santos-Martins, D., Tillack, A. F., and Forli, S. 2021. AutoDock Vina 1.2.0: New Docking Methods, Expanded Force Field, and Python Bindings. *Journal of Chemical Information and Modeling* 61(8): 3891–3898. DOI: 10.1021/acs.jcim.1c00203

Ekamawanti, H. A., Simanjuntak, L., and Muin, A. 2021. Assessment of the Physical Quality of *Eucalyptus pellita* Seedlings from Shoot Cutting by Age Level. *Jurnal Sylva Lestari* 9(2): 280–290. DOI: 10.23960/jsl.v9i2.280-290

Faia, J., Costa, J., Araújo, J., Borralho, N., Marques, C., and Trindade, H. 2022. Impact of Inbreeding on Growth and Development of Young Open-Pollinated Progeny of *Eucalyptus globulus*. *iForest* 15(5): 356–362. DOI: 10.3832/ifor4012-015

Fikry, E., Orfali, R., Tawfeek, N., Perveen, S., Ghafar, S., El-Domiaty, M. M., and El-Shafae, A. M. 2024. Unveiling the Bioactive Efficacy of *Cupressus sempervirens* 'Stricta' Essential

Oil: Composition, *In Vitro* Activities, and *In Silico* Analyses. *Pharmaceuticals* 17(8): 1019. DOI: 10.3390/ph17081019.

Girola, N., Figueiredo, C. R., Farias, C. F., Azevedo, R. A., Ferreira, A. K., Teixeira, S. F., Capello, T. M., Martins, E. G., Matsuo, A. L., Travassos, L. R., et al. 2015. Camphene Isolated from *Piper cernuum* Essential Oil Induces Intrinsic Apoptosis in Melanoma Cells. *Biochemical and Biophysical Research Communications* 467(4): 928–934. DOI: 10.1016/j.bbrc.2015.10.041

Hou, J., Zhang, Y., Zhu, Y., Zhou, B., Ren, C., Liang, S., and Guo, Y. 2019. α-Pinene Induces Apoptotic Cell Death via Caspase Activation in Human Ovarian Cancer Cells. *Medical Science Monitor* 25: 6631–6638. DOI: 10.12659/msm.916419

Hudaib, M., and Aburjai, T. 2007. Volatile Components of *Thymus vulgaris* L. from Wild-Growing and Cultivated Plants in Jordan. *Flavour and Fragrance Journal* 22(4): 322–327. DOI: 10.1002/ffj.1800

Hudaib, M., Bellardi, M. G., Rubies-Autonell, C., Fiori, J., and Cavrini, V. 2001. Chromatographic (GC-MS, HPLC) and Virological Evaluations of *Salvia sclarea* Infected by BBWV-I. *Il Farmaco* 56(3): 219–227. DOI: 10.1016/S0014-827X(01)01038-2

Industry Research Ltd. 2025. *Eucalyptus Oil Market Size, Share, and Forecast to 2035*. Industry Research Ltd.

International Agency for Research on Cancer (IARC). 2024. *Indonesia Fact Sheet: GLOBOCAN 2022*. World Health Organization, Lyon, France. URL: https://gco.iarc.who.int/media/globocan/factsheets/populations/360-indonesia-fact-sheet.pdf. Accessed April 22, 2026.

ISO 3065 (2021). *Essential Oil of Eucalyptus, Australian Type*. International Organization for Standardization, Geneva, Switzerland.

Jo, H., Cha, B., Kim, H., Brito, S., Kwak, B. M., Kim, S. T., Bin, B. H., and Lee, M. G. 2021. α-Pinene Enhances the Anticancer Activity of Natural Killer Cells via ERK/AKT Pathway. *International Journal of Molecular Sciences* 22(2): 656. DOI: 10.3390/ijms22020656

Koursaoui, B., Satrani, M., Ghanmi, M., Cherrad, S., Jaouadi, I., Hajib, S., Aouane, E. M., and Chaouch, A. 2021. *Eucalyptus sideroxylon* A. Cunn.: A Natural Eucalyptol (1,8-Cineole) Source in Morocco. *Research Journal of Pharmacy and Technology* 14(9): 4583–4590. DOI: 10.52711/0974-360x.2021.00797

Li, C., Zha, W., Li, W., Wang, J., and You, A. 2023. Advances in the Biosynthesis of Terpenoids and Their Ecological Functions in Plant Resistance. *International Journal of Molecular Sciences* 24(14): 11561. DOI: 10.3390/ijms241411561

Long, G. V., Stroyakovskiy, D., Gogas, H., Levchenko, E., de Braud, F., Larkin, J., Garbe, C., Jouary, T., Hauschild, A., Grob, J. J., et al. 2014. Combined BRAF and MEK Inhibition Versus BRAF Inhibition Alone in Melanoma. *New England Journal of Medicine* 371(20): 1877–1888. DOI: 10.1056/nejmoa1406037

Lowman, K., Magalhães, M., Lemos, M. F. L., Cabral, C., and Pires, I. M. 2018. Anticancer Properties of Essential Oils and Other Natural Products. *Evidence-Based Complementary and Alternative Medicine* 2018: 3149362. DOI: 10.1155/2018/3149362

Lu, F. L., Chen, Y. Y., Wei, J. H., Huang, Y. L., Li, D. P., and Liu, Z. Y. 2014. Chemical Characterisation of *Eucalyptus* Hybrids and Six Pure *Eucalyptus* Species Grown in Guangxi (China). *Advanced Materials Research* 1033–1034: 200–208. DOI: 10.4028/www.scientific.net/amr.1033-1034.200

Mahumane, G. D., van Vuuren, S. F., Kamatou, G. P. P., Sandasi, M., and Viljoen, A. M. 2016. Chemical Composition and Antimicrobial Activity of *Eucalyptus radiata* Leaf Essential Oil, Sampled Over a Year. *Journal of Essential Oil Research* 28(6): 475–488. DOI: 10.1080/10412905.2016.1175386

Marnaek, R. H., Setiawan, Y., Hermawan, R., and Muhdin. 2024. Development of Allometric Model for Estimating Biomass and Carbon Storage of Hybrid *Eucalyptus* (*Eucalyptus grandis* × *Eucalyptus urophylla*) in Industrial Plantation Forests of North Sumatra Province. *Jurnal Sylva Lestari* 12(4): 948–961. DOI: 10.23960/jsl.v12i4.948-961

Moriarity, D. M., Bansal, A., Cole, R. A., Takaku, S., Haber, W. A., and Setzer, W. N. 2007. Selective Cytotoxic Activities of Leaf Essential Oils from Monteverde, Costa Rica. *Natural Product Communications* 2(12): 1263–1268. DOI: 10.1177/1934578x0700201215

Munawaroh, K., Hafidz, M., Jayani, F. M., Murda, R. A., and Jarwinda. 2025. Utilization of Pulp and Paper Waste as an Ameliorant in Marine Clay Soil to Increase the Growth of *Eucalyptus pellita* F. Muell. *Jurnal Sylva Lestari* 13(3): 662–675. DOI: 10.23960/jsl.v13i3.662-675

Nirsatmanto, A., Sunarti, S., Kartikaningtyas, D., Handayani, B. R., Setyaji, T., Pudjiono, S., Kartikawati, N. K., Kardiansyah, T. E., Indrawan, D. A., Pari, R. O., et al. 2022. Evaluation of *Eucalyptus pellita* and *Acacia* Hybrids. *Wood Research* 67(5): 847–865. DOI: 10.37763/wr.1336-4561/67.5.847865

Prayogo, Y. H., Anggini, A. W., Carolina, A., Manurung, E. G. T., Sari, R. K., Purwoko, A., and Pasaribu, G. 2025. Antibacterial Potency of *Eucalyptus* Leaf Oil from Hybrid Clones of *E. grandis* with *E. urophylla* and *E. pellita*. *Applied Science and Engineering Progress* 18(3): 7671. DOI: 10.14416/j.asep.2025.01.002

Prayogo, Y. H., Wahyudi, T. S., Batubara, I., Sari, R. K., and Syafii, W. 2024. Multitarget Ensemble Docking of Potent Anticancer Compounds. *Research Journal of Pharmacy and Technology* 17(2): 707–716. DOI: 10.52711/0974-360x.2024.00110

Pujiarti, R., Nurjanto, H. H., and Sunarta, S. 2018. Antifungal Activity of *Eucalyptus urophylla* Oil Against *Aspergillus niger* and *Fusarium oxysporum*. *Agrivita Journal of Agricultural Science* 40(1): 55–62. DOI: 10.17503/agrivita.v40i1.990

Purwoko, A., Muhdi, Sari, R. K., Azhar, I., Sianturi, Y. R. U., and Sembiring, H. 2024. The assessment of Essential Oil Potential from waste logging of different *Eucalyptus* Clones in PT Toba Pulp Lestari Tbk's industrial plantation forests, Indonesia. . *Plant Science Today* 11(2): 681–687. DOI: 10.14719/pst.2888

Rajapaksha, C., Apiolaza, L. A., Squire, M. A., and Altaner, C. M. 2023. Genetic Parameters of Essential-Oil Traits for *Eucalyptus bosistoana*. *Australian Forestry* 86(2): 90–99. DOI: 10.1080/00049158.2023.2270681

Susianti, S., Lesmana, R., Salam, S., Julaeha, E., Pratiwi, Y. S., Sylviana, N., Goenawan, H., Kurniawan, A., and Supratman, U. 2021. The Effect of Nutmeg Seed (*Myristica fragrans*) Extracts Induces Apoptosis in Melanoma Maligna Cell's (B16-F10). *The Indonesian Biomedical Journal* 13(1): 68–74. DOI: 10.18585/inabj.v13i1.1424

Van den Berg, K. S., Verryn, S. D., and Naidoo, S. 2015. Genetic Parameters of Interspecific Hybrids of *Eucalyptus grandis* and *Eucalyptus urophylla* Seedlings and Cuttings. *Silvae Genetica* 64(1–6): 291–308. DOI: 10.1515/sg-2015-0027

Vaux, D. L., Fidler, F., and Cumming, G. 2012. Replicates and Repeats—What Is the Difference and Is It Significant? A Brief Discussion of Statistics and Experimental Design. *EMBO Reports* 13(4): 291–296. DOI: 10.1038/embor.2012.36

Wu, Z., Du, Y., Guo, Z., Lei, K., Jia, Y., Xie, M., Kang, X., Wei, Q., He, L., Wang, Y., et al. 2016. Essential Oil and Its Major Compounds from Oil Camphor Inhibit Human Lung and Breast Cancer Cell Growth by Cell-Cycle Arresting. *International Journal of Clinical and Experimental Medicine* 9(7): 12852–12861.

Xu, Q., Li, M., Yang, M., Yang, J., Xie, J., Lu, X., Wang, F., and Chen, W. 2018. α-Pinene Regulates miR-221 and Induces G2/M Phase Arrest in Human Hepatocellular Carcinoma Cells. *Bioscience Reports* 38(6): BSR20180980. DOI: 10.1042/bsr20180980

Yip, S. C., Ho, L. Y., Wu, T. Y., and Sit, N. W. 2024. Chemical Composition and Bioactivities of *Eucalyptus* Essential Oils from Selected Pure and Hybrid Species: A Review. *Industrial Crops and Products* 222: 120118. DOI: 10.1016/j.indcrop.2024.120118

Zhou, L., Li, J., Kong, Q., Luo, S., Wang, J., Feng, S., Yuan, M., Chen, T., Yuan, S., and Ding, C. 2021. Chemical Composition and Bioactivity of *Eucalyptus* Oils. *Molecules* 26(5): 1450. DOI: 10.3390/molecules26051450

Zhong, W., Myers, J. S., Wang, F., Wang, K., Lucas, J., Rosfjord, E., Hooper, A. T., Yang, S., Lemon, L. A., et al. 2020. Comparison of the Molecular and Cellular Phenotypes of Common Mouse Syngeneic Models with Human Tumors. *BMC Genomics* 21(2): 1–17. DOI: 10.1186/s12864-019-6344-3

Zhu, Y., Wu, S., Xu, J., Lu, Z., Li, G., Hu, Y., Yang, X., and Bush, D. 2017. Genetic Parameters for Growth Traits and Stem-Straightness in *Eucalyptus urophylla* × *Eucalyptus camaldulensis* Hybrids from a Reciprocal Mating Design. *Euphytica* 213: 142. DOI: 10.1007/s10681-017-1923-3